Evaluation of Material Plate Proprieties Using Inverse Problem NDT Techniques

M. CHEBOUT[1], A.SADOU, L. AOMAR, M.R.MEKIDECHE
E-mail chebout_med@yahoo.fr
[1] Laboratoire d'Etudes et de Modélisation en Electrotechnique, Université de Jijel, Algérie

Abstract — The defect detection mechanism for eddy current non-destructive testing (NDT) probes is related to the interaction of induced eddy currents in the metal test specimen with flaws and the coupling of these interaction effects with the moving test probe. We review in this paper formulation of three dimensional eddy current problems in terms of various magnetic and electric potentials in order to predict change in impedance of an absolute coil as it scans the metal plate surface along the diagnostic direction for detection of flaws and than evaluate characterization of material using BFGS optimisation method.

***Keywords*—Non-destructive testing, Normalized impedance diagram, Inverse problem, BFGS method, Optimization**

I. INTRODUCTION

Eddy current non destructive testing (NDT) of conducting materials is of importance in many domains of industry: energy production (nuclear plants), transportation (aeronautic), workpiece manufacturing, etc. This technique based on the analysis of changes in the impedance of one or more coils places near the workpiece to be tested, is used to detect and characterize possible flaw or anomalies in the workpiece.

In recent years, with strong requirement for structural safety, eddy current testing has progressed to a quantitative detection stage[1]. Shapes and localisation of defects are required for the assessment of defect propagation and determination of critical flaws. Encouraging results were achieved for the reconstruction of a single crack in the case when the detecting probe scans just over the crack.

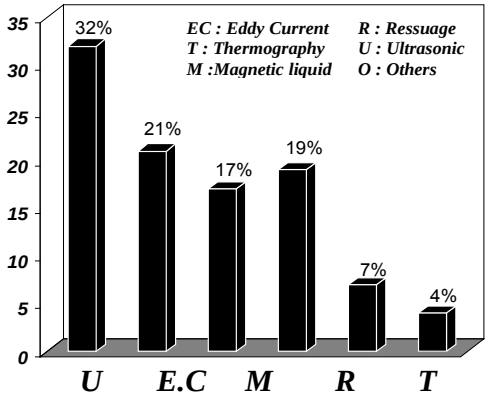

Fig.1 non destructive testing methods distribution

A comparison between various diagnostic methods is shown in Fig.1 [2]**.** A typical eddy current problem is depicted in Fig.2. It consists of an eddy current region with nonzero conductivity Ω_C and a surrounding region free of eddy currents which may, however, contain source currents Ω_j [3]

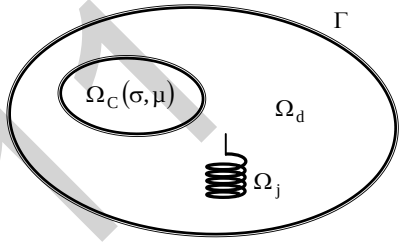

Fig 2 : Eddy current non destructive Problems

A number of approach already exists to model the interaction between the probe and the tested structure. The most general ones in complex geometries use the numerical methods. In this paper, we describe such a computational model that uses the finite element method for calculating eddy current probe signals due to cracks. In earlier studies, the calculations were performed for planar structures [1]

II. FINITE ELEMENT METHOD FORMULATION

The treatment of the eddy current problem is based on the solution of one or more differential equations derived from Maxwell's equations under the general assumption that the displacement current density, in conducting media may be neglected for lower frequencies.[1][3]

In three-dimensional eddy current problems, both the electric and the magnetic filed must be described in conductors, the electromagnetic field in this case can be derived from potentials using the magnetic vector potential and the electric scalar potential, while in eddy current-free regions it suffices to make into account the magnetic field only.

The time-harmonic eddy current problem is expressed by:

$$\left.\begin{aligned}\nabla\times\left(\frac{1}{\mu}\nabla\times\vec{A}\right)+j\omega\sigma\vec{A}++\sigma\nabla V=0\\ \nabla\cdot\sigma\left(j\omega\vec{A}+\nabla V\right)=0\end{aligned}\right\}\ \text{in}\ \Omega_C \qquad (1)$$

$$\nabla\times\left(\frac{1}{\mu}\nabla\times\vec{A}\right)=J \qquad \text{in}\ \Omega_j \qquad (3)$$

Where J the external current density, μ is the permeability, σ is the conductivity of conductive materials and ω is the angular frequency of the excitation source. The magnetic vector potential is not uniquely defined by the equations (1) and (2) when both filed $\vec{J}$ and $\vec{B}$ are automatically forced to be solenoidal. To ensure the uniqueness of the potentials, we need to impose further requirements, i.e. the gauge conditions together with the correct selection of boundary conditions.

There are several possible ways to treat the uniqueness of the magnetic vector potential. The most popular is the coulomb gauge:

$$\nabla \vec{A} = 0 \tag{4}$$

One of the effective and widely used methods of numerically computing eddy current fields in three dimensions is the finite element method. In this paper, nodal finite elements only are considered where the unknown scalar and /or vector functions, the potentials, are approximated by interpolating their values in the nodes of the finite elements [1].

Using finite element Galerkine techniques, the Dirichlet boundary conditions require nodal potentials to be set to the known values. The Newman boundary conditions can be satisfied in a natural way. This is illustrated for the case of the magnetic vector potential and the electric scalar potential writing the Galerkin weak form of Equ.(1) And (2). With $\vec{W}$ and W denoting the weighting functions which coincide with the shape functions in a finite element realisation. Then (1) and (2) are replaced by:

$$\int_\Gamma \vec{W} \cdot \nabla \times \left(\frac{1}{\mu} \nabla \times \vec{A} \right) d\Gamma + \int_\Gamma j\sigma\omega \vec{A} \vec{W} d\Gamma + \sigma \vec{W} \int_\Gamma \nabla V d\Gamma = 0 \tag{5}$$

$$\int_\Gamma W \nabla \cdot \sigma \left(j\omega \vec{A} + \nabla V \right) d\Gamma = 0 \tag{6}$$

Using the gauss's theorem, (5) becomes:

$$\int_\Gamma \left(\frac{1}{\mu} \nabla \times \vec{W} \right) \cdot \nabla \times \vec{A} \, d\Gamma + \oint_S \vec{W} \cdot \left(\frac{1}{\mu} \nabla \times \vec{A} \times \vec{n} \right) dS + \int_\Gamma j\omega\sigma \vec{W} \cdot \vec{A} \, d\Gamma + \int_\Gamma \sigma \vec{W} \cdot \nabla V \, d\Gamma = 0 \tag{7}$$

Where S is the surface which encloses V and $\vec{n}$ is the unit normal vector.[4]. After the two magnetic vector and the electric scalar potential are solved, we can calculate the impedance of the coil taken as follow:

$$Z = R + j\omega L \tag{8}$$

Where R is the coil resistance and L is the coil inductance.

The resistance is linked with the dissipated energy P in the conductor in the form of:

$$R = P / I^2 \tag{9}$$

While the inductance is linked with the total stored energy W in the whole solution domain by:

$$L = 2W / I^2 \tag{10}$$

Where I is the external current density, P and W can be expressed by:

$$P = \int_\Gamma \vec{J}\vec{E}^* d\Gamma \quad \text{and} \quad W = \frac{1}{2} \int_\Gamma \vec{H}\vec{B}^* d\Gamma \tag{11}$$

Respectively. Here $\vec{E} = -\nabla V - j\omega \vec{A}$ is the electric field intensity, $\vec{B} = \nabla \times \vec{A}$ is the magnetic flux density, $\vec{H} = \vec{B} / \mu$ is the magnetic field intensity, Γ refers to the solution domain, and * denotes the complex conjugate operator.[4][5].

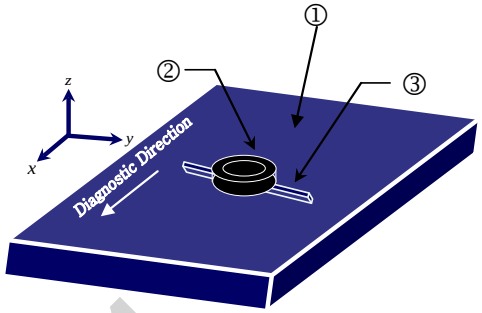

Fig 3 representation of the 3D benchmark EC geometry

We solve a benchmark model of eddy current testing [6]. We analyze eddy currents of a metal plate $(140 \times 140 \times 1.25\,mm)$ with a crack $(10 \times 0.2 \times 0.75\,mm)$ as shown in Fig.1. Conductivity and relative permeability of the plate are $\sigma = 1\,MS/m$ and $\mu_r = 1$. An exciting coil with 140 turns is placed above the crack. Inner and outer diameters of the coil are $r_1 = 1.2\,mm$ and $r_2 = 3.2\,mm$, the height of the coil is $h = 0.8\,mm$. The current of the coil is equivalent to $I_c = 1/140\,A$ and the work frequency is $fr = 300\,kHz$. The gap between the lower surface of the coils and the upper surface of the plate named lift-off $(l_{lift-off})$ distance is equal to $L = 0.5\,mm$

TABLE 1 SPECIFICATION OF THE MODEL

	Item	Value
Conductive plate ①	Plate conductivity	$1 \times 10^6\,[S/m]$
	Plate thickness	1.25[mm]
	Plate length	140 [mm]
	Plate width	140 [mm]
	Frequency	300 [kHz]
Coil ②	Coil inner radius	0.60 [mm]
	Coil outer radius	1.60 [mm]
	Coil height	0.80 [mm]
	Coil Lift-off	0.50 [mm]
Crack ③	Crack width	0.2 [mm]
	Crack length	10 [mm]
	Crack depth	0.75[mm]

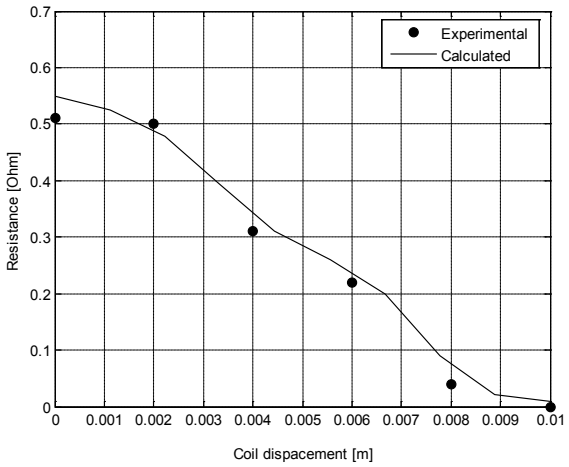

Fig 4 Experimental and calculated resistance components as function as coil displacement

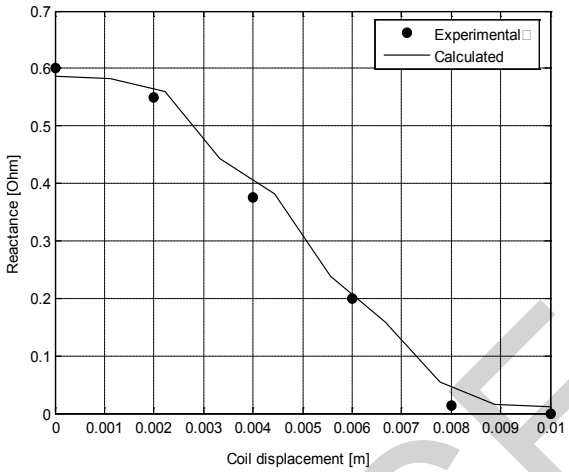

Fig 5 Experimental and calculated reactance components as function as coil displacement

The impedance change represented by the resistance and the reactance components in Figs. 4 and 5, is evaluated by subtracting the values obtained for the plate without rectangular-shape crack from the values obtained for the plate with crack. These parameters are calculated at frequencies of 300 kHz for lift-offs of 0.5mm at different coil locations with a 1mm displacement step. A preconditioning technique, called the symmetric successive over-relaxation (SSOR) method is employed to minimize computation time and memory.

In figure 6 we show decrease in relative error as function as iterations. She indicate that symmetric successive over-relaxation (SSOR) method employed to solve electromagnetic equations converge to initial value equal to $\varepsilon = 10^{-9}$.

The coil impedance $Z = R + jX$ is the typical of eddy current distribution in the material. In order to eliminate the influence of the electrical proprieties of the coil itself, the normalized impedance has been calculated:

$$R_n = (R - R_0)/R_0 \quad (12)$$

$$X_n = X / X_0 \quad (13)$$

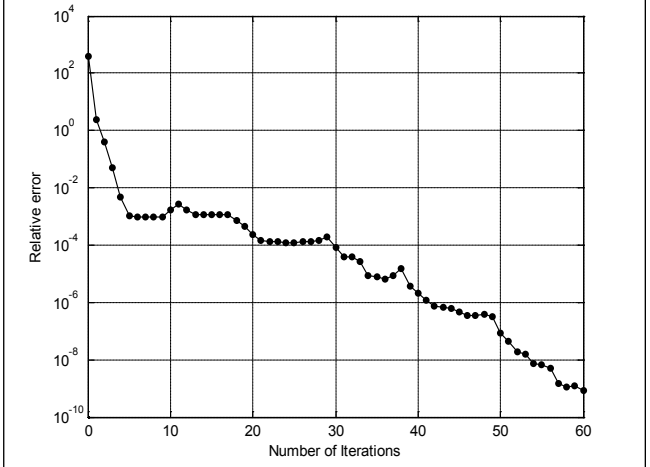

Fig. 6 Relative error as function as number of iterations

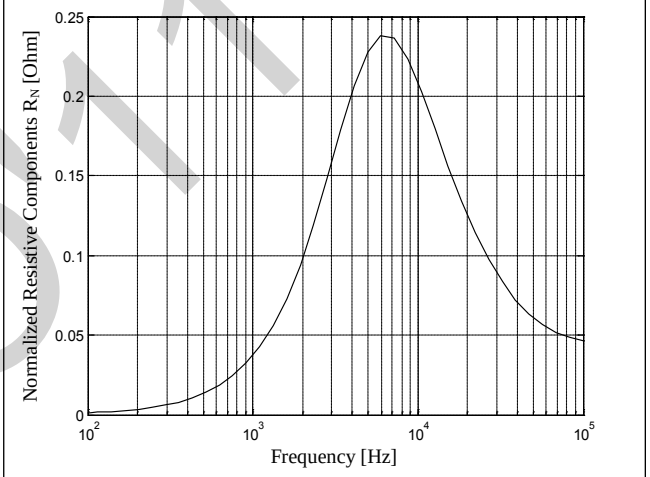

Fig 7 Normalized resistance components as function as frequency

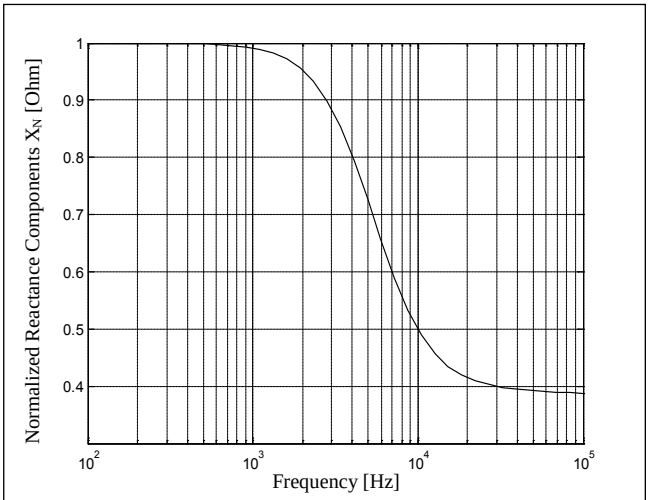

Fig 8 Normalized reactance components as function as frequency

Where R_n is the normalized resistive component, and X_n represent the normalized reactive component [2][6].

On the one hand, we illustrate in Fig.7 variation of real part of normalized impedance as function as frequency and on the other hand, we illustrate in Fig.8 variation in imaginary part of normalized impedance versus frequency.

We illustrate in figure 9 normalized impedance plane diagrams which consist to plot the real part as functions as the imaginary part of normalized impedance for thirteen values of frequency distributed between 100 Hz and 1MHz for three different depth defect values: at surface of conductive plate, at 0.1 mm, and at 0.20 mm from a conductive plate surface as shown in Fig.9. We remark decreasing in values of the two parts of normalized impedance when distance d_0 increase.

There is relationship between the coupling coefficient and the impedance diagram. This relationship is given by $K^2 = 1 - X_c$.

Where K is the coupling coefficient and X_c, is the value of the reactance at the point where the normalized impedance curve, extrapolated to high frequency or conductivity, intersects the ordinate axis.

In Fig 10, we show idealized real component as function as idealized imaginary component of impedance given as follows:

$$X_{nn} = \frac{X_n - X_c}{1 - X_c} = \frac{X_n + K^2 - 1}{K^2} \quad (14)$$

and

$$R_{nn} = \frac{R_n}{K^2} \quad (15)$$

The Lift-off influence is currently considered in eddy current non destructive testing method. As lift-off is increased the electromagnetic coupling between the probe and the test material decreases as there is greater flux leakage, and the size of the impedance diagram decreases.

To determine Lift-off angle, we considered the parameter θ_L given as:

$$\tan\theta_L = \frac{1 - X_c}{R_n} \quad (16)$$

Figure 11 illustrate Lift-off angle as function as $\frac{r}{\delta}$ where r represent the mean coil radius and δ is the skin depth.

In order to evaluate the limits of flaw detection we considered the notion of ΔR_n and ΔX_n where:

$$\Delta R_n = R_n(Unflawed) - R_n(flawed) \quad (17)$$

$$\Delta X_n = X_n(Unflawed) - X_n(flawed) \quad (18)$$

We plot variation in normalize impedance components for four depth defect values: at surface of conductive plate, at 0.05 mm,0.10mm and at 0.15 mm from a plate surface as shown in figure 12 (for variation in imaginary parts) and figure 13 (for variation in imaginary parts) of normalized impedance.

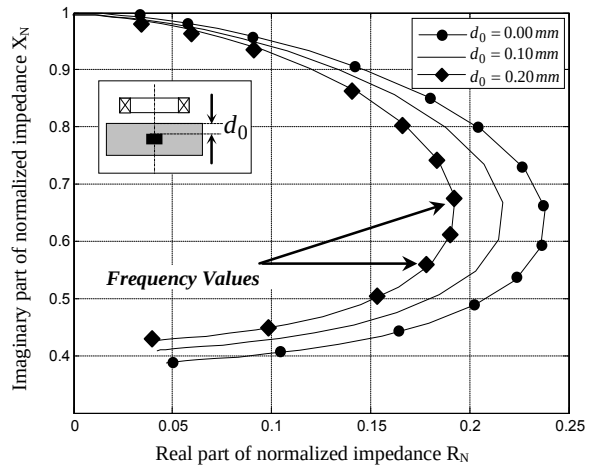

Fig 9 Normalized impedance plane diagrams for different cracks depth d_0

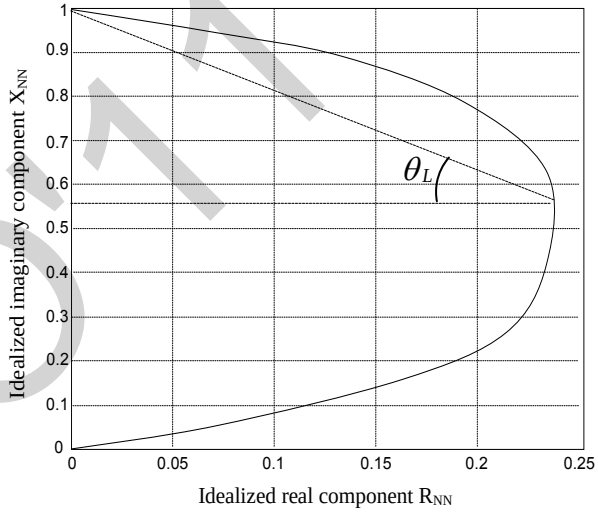

Fig 10 Idealize Normalized impedance plane diagrams

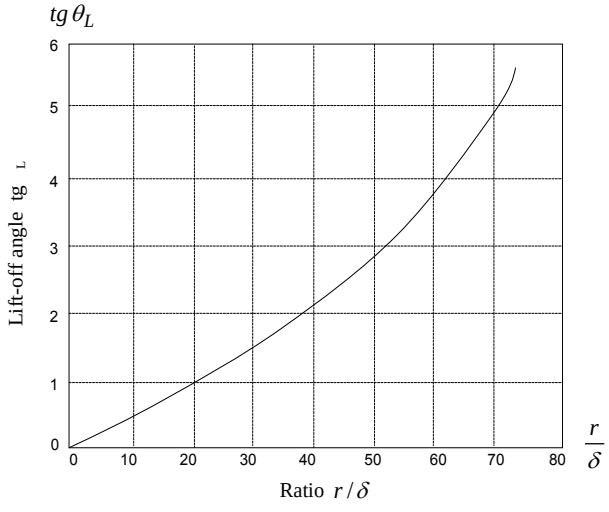

Fig.11 Lift off angle as function as r/δ

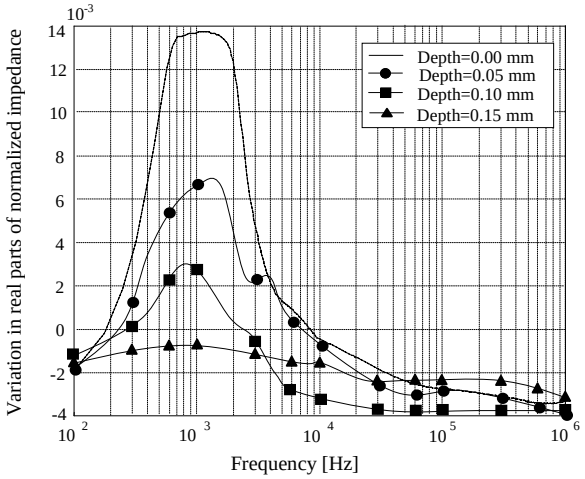

Fig 12 Variation in real parts of normalized impedance as function as frequency

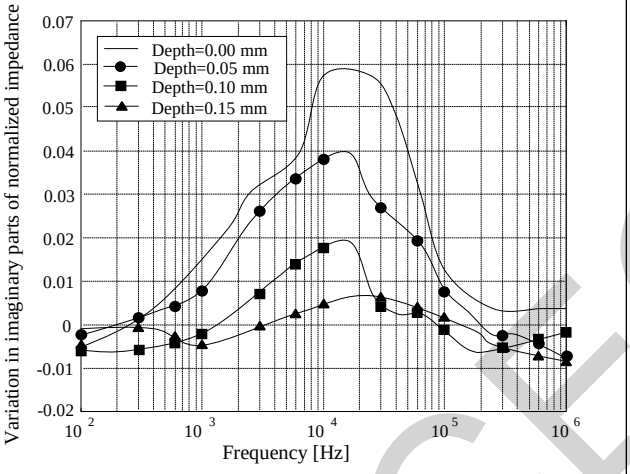

Fig 13 Variation in imaginary parts of normalized impedance as function as frequency

In order to characterize a conductive plate we need an objective function, which minimizes the mean-square difference between tentative predictions of the probe signals and the measurements. In this case the key's function is variation in impedance showing as follows:

$$f = \sum_{i=1}^{n} \left| \Delta Z^{i} - \Delta Z_{meas}^{i} \right|^{2} \qquad (19)$$

Where n denote the number of measured points, and the superscript "i" is equivalent to the $i^{(th)}$ observation point.

If the agreement is unsatisfactory, then the problem is updated and a new prediction is made. The process continues through a number of iterations until predictions and observations match to within a reasonable tolerance.

In Fig.14 we show evolution of objective function f as function as number of iterations equal to 100 iterations. We observe that the difference between calculated impedance and measured impedance decrease satisfying relation (19).

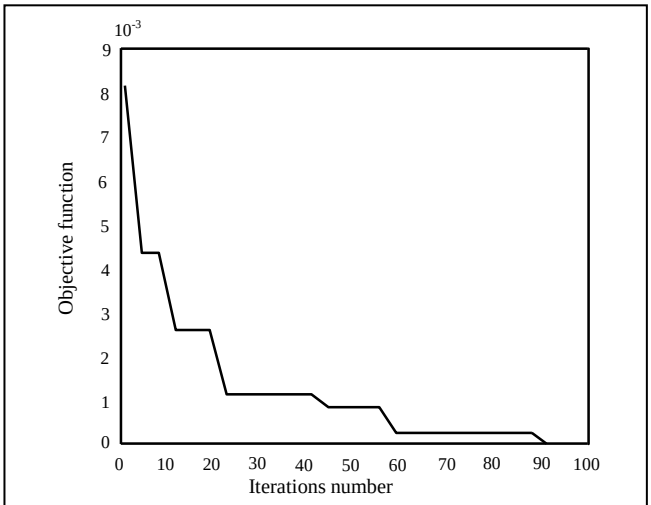

Fig 14 Evolution of Objective function versus iterations number

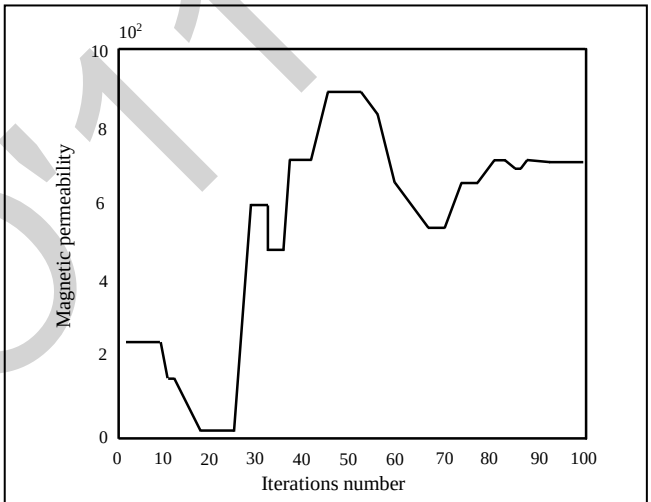

Fig 15 Evolution of Magnetic permeability as function as iterations number

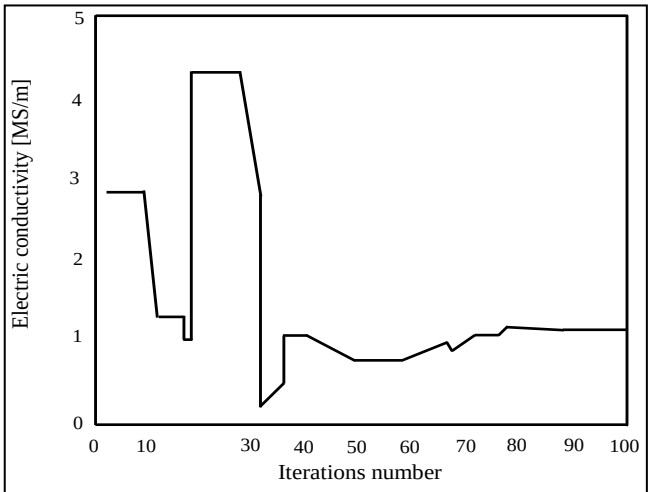

Fig 16 Evolution of electric conductivity as function as iterations number

Magnetic permeability and electrical conductivity showing in Fig.15 and Fig.16 respectively meet to the optimum values.

We remark a good agreement between obtained and expected parameters of the conductive material which is a benefit to BFGS optimization method.

III. CONCLUSION

The aim of this paper is to show three dimensional finite elements modelling and material characterization using BFGS optimization method by calculation magnitude impedance along a diagnostic direction and variation in normalized components such as normalized resistive components and normalized imaginary components as function as frequency for different depths crack.

In the first, we obtained a good agreement between calculated impedance components and experimental data witch is considered as a validation of our theoretical results.

Then, we calculate normalized impedance components as function as frequency and obtained normalized plane diagrams by showing effect of depths defect in non-destructive operation.

After that, BFGS optimisation method is employed to characterize material proprieties such as magnetic permeability and electrical conductivity.

IV. REFERENCES

[1] O. Biro and K.Preis, " On the use of the magnetic vector potential in the finite element analysis of three dimensional eddy currents''. *IEEE, tansactions on magnetics* Vol 25, N°04, July 1989.

[2] S. Bakhtiari and D.S.Kupperman, " Modeling of eddy current probe response for steam generator tubes", *Nuclear enginnering and design*. 1999, pp, 57-71.

[3] E.E.Kriezis, T.D.Tsiboukis, S.M.Panas, J.A.Tegopoulos "Eddy current: theory and applications". *Proceeding of the IEEE,* Vol,80, N°10, December 1992.

[4] G.Pichnot, T.Sollier. "Eddy current modelling for non destructive testing". *8th European conference in non destructive testing*, June 17-21 2002.

[5] O.Biro, I.Bardi, K.Preis, K.R.Richter, "Compulation of 3D electromqgnetic filed by finite element" *Journal of physic III*, pp 1971-1977, November 1992.

[6] Y.Bihan "3D finite element analysis of eddy current evaluation of curved plates" *IEEE, tansactions on magnetics*. Vol 38, N°02, march 2002.